Preprints of the 21st IFAC World Congress (Virtual)
Berlin, Germany, July 12-17, 2020

Inferential control of product properties for fluidized bed spray granulation layering

Robert Dürr * **Christoph Neugebauer** ** **Stefan Palis** **,***
Andreas Bück **** **Achim Kienle** *,**

* *Max Planck Institute for Dynamics of Complex Technical Systems, Magdeburg, 39106, Germany (e-mail: duerr@mpi-magdeburg.mpg.de).*
** *Otto von Guericke University, Magdeburg, 39106, Germany*
*** *Moscow Power Engineering Institute (MPEI), Moscow, Russia*
**** *Friedrich Alexander University, Erlangen, 91058, Germany*

Abstract: Fluidized bed layering granulation has found application in a wide range of industrial processes, e.g. food, pharmaceutical or fertilizer manufacturing. The quality of the produced granules is a critical factor for subsequent processing steps and depends on individual particle properties like characteristic size, porosity or mechanical stability. Therefore, these properties have to be monitored closely during the process to enable accurately timed intervention by plant operators or the application of suitable feedback control algorithms. In case certain properties are not measurable due to financial or technical limitations, observer techniques can fill the gap and provide reliable estimates for these properties. In this manuscript, observer design is demonstrated and validated for a fluidized bed layering granulation process model represented by a complex set of partial and ordinary differential equations. Furthermore, an inferential integral state feedback controller is designed and applied to the complex nonlinear model.

Keywords: Distributed parameter systems, continuous fluidized bed layering granulation, state estimation, model-based control

1. INTRODUCTION

Fluidized bed layering granulation (FBLG) represents an established particle formation process which has found broad industrial application, e.g. food, pharmaceutical or fertilizer manufacturing, for the production of high quality granules (Mörl et al., 2007; Litster and Ennis, 2004). Therein, a solid-containing liquid is sprayed on an ensemble of fluidized particles forming droplets or a liquid layer on the particle surface. As the fluidization medium is heated, the liquid part is removed by evaporation resulting in a layer wise growth of the granules. The obtained particles are generally easier to handle than their liquid equivalent and specific particle properties may be required for subsequent processing steps. Furthermore, operation in continuous mode, e.g. by using sieve-mill recycle streams (see Fig. 1) enables high throughput.

It is well known that the product quality is significantly affected by operating conditions (Neugebauer et al., 2018), motivating application of feedback-control algorithms (Bück et al., 2016; Cotabarren et al., 2015) to guarantee constant product quality. Those generally require online-measurement of the corresponding particle properties, e.g. characteristic particle size, using sophisticated sensor techniques which rely on assumptions on the particle shape, e.g. sphericity. If these assumptions do not hold, e.g. in case of non spherically shaped particles, the measurements become unreliable. Moreover, measurements of particle properties of interest may not even be available due to financial or safety restrictions. In such cases, the desired information can be inferred from available or more

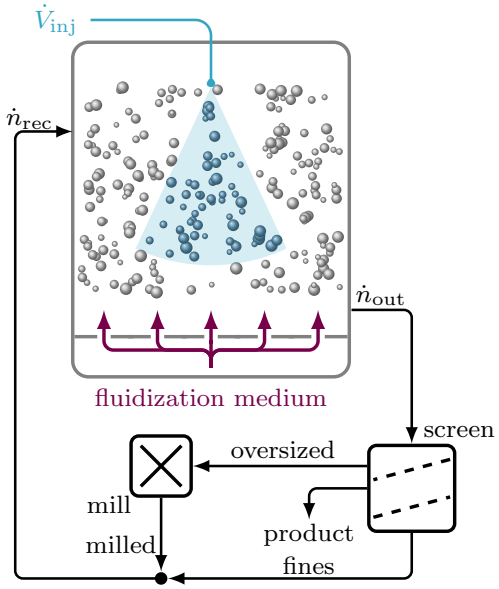

Fig. 1. *Scheme of spray fluidized bed layering granulation (FBLG) process with sieve-mill recycle*

reliable measurements using a model of the process, which is also known as observer approach (Mohd Ali et al., 2015; Dürr and Waldherr, 2018).

In this contribution, we will present design and evaluation of observers and observer-based (inferential) controllers for a continuously operated spray FBLG process. In the following, process modeling, observer and controller design,

as well as numerical evaluation of the methods will be presented subsequently.

2. PROCESS MODELING

Fluidized-bed layering granulation in the described operation mode represents a complex process which is affected by the coupling of the particle phase to the fluidization medium. A sophisticated mathematical model accounting for mass and heat transfer phenomena as well as evolution of the heterogeneous particle ensemble in the fluidization chamber is found in Neugebauer et al. (2018) and roughly consists of two major parts: The first part is a population balance model (Ramkrishna, 2000), which characterizes the dynamics of the particle size number density distribution

$$\frac{\partial n(t,L)}{\partial t} + G\frac{\partial n(t,L)}{\partial L} = \dot{n}_{rec}(t,L) - \dot{n}_{out}(t,L)\,. \qquad (1)$$

Here, the particle size number density distribution $n(t,L)$ describing the density of particles within a infinitesimal size-class, changes by growth of particles, represented by growth rate G, reflux of milled oversized and undersized particles $\dot{n}_{rec}$ as well as withdrawal of particles from the chamber $\dot{n}_{out}$. The disperse solid (particle) phase is coupled to a system of ordinary differential equations representing the temporal evolution of thermal properties such as particle and fluidization gas temperature, θ_p and θ_f, particle and fluid moisture, X and Y via coupled mass and enthalpy balances of the solid and gas phase. Bidirectional coupling of both parts, disperse solid (particle) phase and thermal conditions becomes obvious in Fig. 2. The interested reader is referred to the original publication (Neugebauer et al., 2018) for the detailed model. The overall surface of the particles

$$A_{bed} = \pi \int_0^\infty L^2 n(t,L)\mathrm{d}L \qquad (2)$$

affects heat transfer $\dot{Q}_{fp}$ and thereby evaporation of the solvent. The latter is modelled with a tri-stage evaporation model (van Meel, 1958) in the presented model formulation. Heat and mass transfer affect the moistures of the particles and fluid X and Y as well as the fluid and particle temperatures θ_f and θ_p. Moreover, the thermal states affect the average particle shell porosity ϵ_{shell} and drying potential

$$\eta = \frac{Y_{sat} - Y}{Y_{sat} - Y_{in}}\,. \qquad (3)$$

Therein, the saturated moisture content of the fluid Y_{sat} directly depends on the current fluid temperature. Milling degree and drying potential directly affect the milling process and the growth velocity, thereby coupling the thermal properties to the disperse phase.

From the industrial side of view there is usually more interest in a few characteristic quantities of the heterogeneous particle ensemble instead of information on the full distribution $n(t,L)$ itself. In industrial practice, the Sauter mean diameter

$$d_{32} = \frac{\int_0^\infty L^3 n(t,L)\ \mathrm{d}L}{\int_0^\infty L^2 n(t,L)\ \mathrm{d}L} \qquad (4)$$

is commonly used as a characteristic integral property of the particle ensemble. Furthermore, Rieck et al. (2015) showed that η is directly related to the average particle porosity. In the following, Sauter mean diameter and drying potential will therefore represent the quality of manufactured granules. It was also shown in Neugebauer et al. (2018) that both can be influenced by manipulation of the average milling degree μ_{mill} and the fluidization gas inlet temperature $\theta_{f,in}$. It was furthermore demonstrated that specific operation regions of those parameters give rise to complex nonlinear phenomena, e.g. sustained oscillations, which are undesired in practice. Hence, those process variables can be viewed as appropriate potential manipulated variables for a feedback control scheme that aim to ensure stable process operation and desired product properties.

3. PROCESS OBSERVER AND CONTROL DESIGN

As an alternative to complex nonlinear infinite-dimensional control design, linear design techniques can be applied to the process in the vicinity of an operation point. In a previous publication (Neugebauer et al., 2020), the complex process model described above is linearized numerically around the operation point

$$\mu_{mill}^{OP} = 0.8\ \mathrm{mm}\,, \quad \theta_f^{OP} = 80^\circ\mathrm{C} \qquad (5)$$

to describe the effects of the manipulated variables μ_{mill} and $\theta_{f,in}$ on the Sauter mean diameter $d_{32}(t)$ and the drying potential $\eta(t)$. The resulting state-space-system obtained after model reduction by balanced truncation (Skogestad and Postlethwaite, 2007) comprises eight states given as

$$\begin{aligned} \dot{x}(t) &= A\ x(t) + B\ u(t)\,, \\ y(t) &= C\ x(t) + D\ u(t)\,, \\ u(t) &= [\Delta\mu_{mill}(t), \quad \Delta\theta_{f,in}(t)]^T\,, \\ y(t) &= [\Delta d_{32}(t), \quad \Delta\eta(t)]\,, \\ A \in \mathbb{R}^{n\times n}\,,\ B \in \mathbb{R}^{n\times m}\,,\ C \in \mathbb{R}^{p\times n}\,,\ D \in \mathbb{R}^{p\times m}\,, \end{aligned} \qquad (6)$$

where the Δ-variables describe the deviation from the operation point and

$$D = [D_{d_{23}},\, D_\eta]^T = \mathbf{0}\,. \qquad (7)$$

For the remainder of the publication it is assumed that d_{32} can not be measured reliably and thus the output equation is given as

$$y(t) = \Delta\eta = C_\eta\ x(t)\,. \qquad (8)$$

It can furthermore be shown that the resulting linear system is observable and controllable.

3.1 State estimation

In order to apply sophisticated control methods, the current value of d_{32} has to be reconstructed from the available measurement of η using a convenient technique like Kalman filtering (Simon, 2006), Luenberger or Sliding mode observers (Shtessel et al., 2014).

In this work a linear quadratic Luenberger observer

$$\begin{aligned} \dot{\widehat{x}}(t) &= A\ \widehat{x}(t) + B\ u(t) + L\ \ (y(t) - \widehat{y}(t)) \\ \widehat{y}(t) &= C_\eta\ \widehat{x}(t) \end{aligned} \qquad (9)$$

was designed with dynamics of estimation error $\widetilde{x} = x - \widehat{x}$ Here, the observer feedback gain L minimizes the quadratic cost function

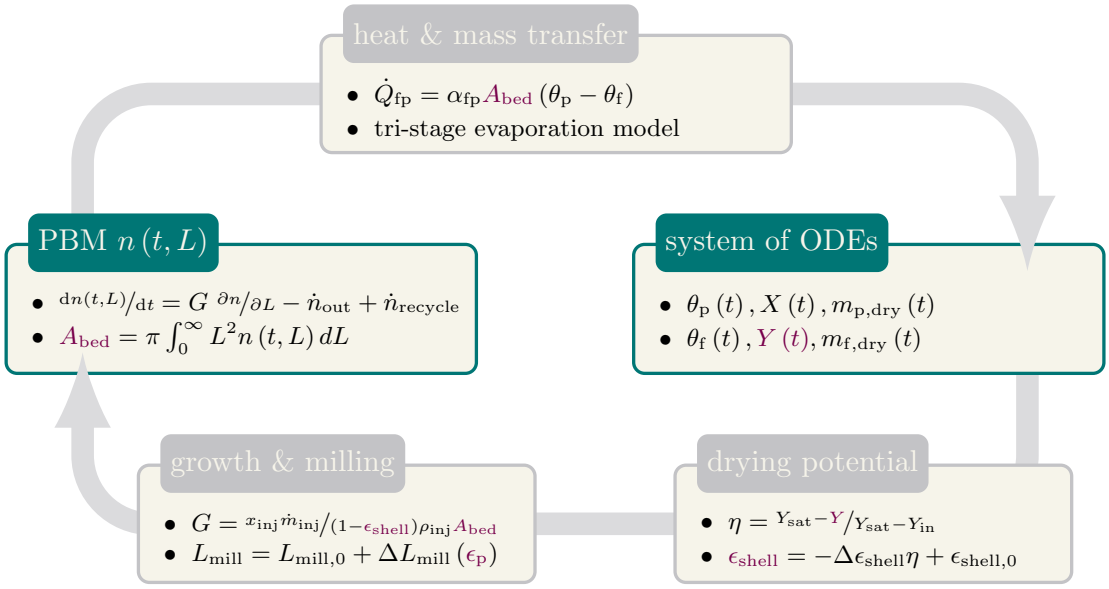

Fig. 2. *Scheme of Model realising coupling between particulate phase (PBM) and thermal conditions (ODEs) via heat/mass transfer and effect of drying potential on particle growth rate*

$$J = \int_0^\infty \tilde{x}^T(t)\ Q\ \tilde{x}(t) + (y(t) - \hat{y}(t))^T(t)\ R\ (y(t) - \hat{y}(t))\mathrm{d}t \tag{10}$$

and is computed from the solution of the associated algebraic Riccati equation. To obtain uniform fast convergence of the states the weighting matrices are chosen as

$$\begin{aligned} Q_{Lue} &= 100 \cdot I^{(8\times 8)} \\ R_{Lue} &= 0.001\,. \end{aligned} \tag{11}$$

It is well known that output estimates from Luenberger type observers may fail to converge in presence of disturbances and plant-model-mismatch. Alternatively, Sliding mode observers (Shtessel et al., 2014) apply nonlinear (switching) output errors estimation feedback and force the the output estimation error to zero in finite time. This could prove advantageous in case of modeling errors or disturbances. The design is described in more detail in the following. Given the system (6) the following coordinate transform is considered

$$z = T_C\ x = \begin{bmatrix} N_C^T \\ C \end{bmatrix}\ x \tag{12}$$

with the transformation matrix $T_C \in \mathbb{R}^{n\times(n-p)}$ and N_C spanning the nullspace of C. The sliding mode observer is now designed in the transformed coordinates with dynamics given by

$$\begin{aligned} \frac{\mathrm{d}}{\mathrm{d}\ t}\begin{bmatrix}\hat{z}_1(t)\\ \hat{z}_2(t)\end{bmatrix} &= \bar{A}\begin{bmatrix}\hat{z}_1(t)\\ \hat{z}_2(t)\end{bmatrix} + \bar{B}\ u(t) + G^{SMO}\ \nu(t) \\ \hat{y}(t) &= \bar{C}_\eta\ \begin{bmatrix}\hat{z}_1(t)\\ \hat{z}_2(t)\end{bmatrix}\,. \end{aligned} \tag{13}$$

Here, the matrices are defined as

$$\begin{aligned} \bar{A} &= T_C A T_C^{-1} = \begin{bmatrix} \bar{A}_{11}^{(n-p)\times(n-p)} & \bar{A}_{12}^{(n-p)\times p} \\ \bar{A}_{21}^{p\times(n-p)} & \bar{A}_{22}^{p\times p} \end{bmatrix} \\ \bar{B} &= T_C B = \begin{bmatrix} \bar{B}_1^{(n-p)\times m} \\ \bar{B}_2^{p\times m} \end{bmatrix}\,, \\ \bar{C}_\eta &= C_\eta \cdot T_C^{-1} = \left[0^{p\times(n-p))},\, I^{p\times p}\right]\,, \end{aligned} \tag{14}$$

$$G_{SMO} = \begin{bmatrix} L^{(n-p)\times p} \\ -I^{p\times p}\,. \end{bmatrix} \tag{15}$$

Further, the state estimation and output errors are defined as

$$e = \hat{z} - z\,, \quad e_y = \hat{y} - y \tag{16}$$

and the nonlinear discontinuous output error injection is approximated by an arctan function

$$\begin{aligned} \nu_i(t) &= \rho\ sign\,(e_{y,i}(t)) = \rho \frac{e_{y,i}(t)}{|e_{y,i}(t)|} \\ &\approx \rho\ \arctan e_{y,i}(t)\,, \\ & i = 1, \ldots, p \end{aligned} \tag{17}$$

For the reduced dynamics on the sliding surface $e_y(t) = 0$,

$$\frac{\mathrm{d}}{\mathrm{d}\ t}(\hat{z}_1 - z_1) = \dot{e}_1(t) = (A_{11} + L\ A_{21})\, e_1(t) \tag{18}$$

with a linear quadratic Luenberger observer with gain L is designed. As for the general Luenberger observer described previously, fast and uniform convergence of the states is desired. The nonlinear gain and the weighting matrices are chosen as

$$\begin{aligned} \rho &= 6.389 \cdot 10^{-5} \\ Q_{SMO}^{obs} &= 100 \cdot I^{(7\times 7)} \\ R_{SMO}^{obs} &= 0.001\,. \end{aligned} \tag{19}$$

3.2 Output feedback

First, the performance is assessed for output feedback control of the Sauter mean diameter d_{32} and drying potential $\eta(t)$ using either direct measurement or an observer-based reconstruction of the former. The controller proposed by

Neugebauer et al. (2020) represents a cascade of two individual PI-controllers given as

$$\begin{aligned}\mu_{mill}(t) &= K_{P,1} \cdot (d_{32,ref}(t) - d_{32}(t)) \\ &\quad + K_{I,1} \int_0^t (d_{32,ref}(\tau) - d_{32}(\tau))\ \mathrm{d}\tau\,, \\ \theta_f(t) &= K_{P,2} \cdot (\eta_{ref}(t) - \eta(t)) \\ &\quad + K_{I,2} \int_0^t (\eta_{ref}(\tau) - \eta(\tau))\ \mathrm{d}\tau\,. \end{aligned} \tag{20}$$

3.3 Integral state feedback

As an alternative to frequency domain-based feedback control design for the spray FBLG process (Neugebauer et al., 2020), integral state-feedback can be considered (Aström and Murray, 2010) with the controller output given as

$$u(t) = -K_s\ \hat{x}(t) - K_i \int_0^t e(\tau)\ \mathrm{d}\tau + K_r\ r(t)\,. \tag{21}$$

Therein, $r(t)$ denotes the desired value of the output variable vector $y(t)$ and the control error is given as $e(t) = r(t) - y^*(t)$ with

$$y^*(t) = \left[\hat{d}_{32}(t)\,, \eta(t)\right]^T\,. \tag{22}$$

In this manuscript, prefilter gain matrix K_r was set to zero as the manipulated variables showed tendencies of increased oscillating behavior. State feedback K_s as well as integral feedback gain K_i are determined by linear quadratic regulator design for the augmented state-space-system. The weighting matrices are chosen as

$$\begin{aligned} Q_{con} &= 5 \cdot diag\left([1,1,1,1,1,1,1,1,1,5]\right) \\ R_{con} &= diag\left(\left[10^7 10^6\right]\right) \end{aligned} \tag{23}$$

to prevent manipulated and systems variables from over- and undershooting maximum and minimum values described in the full nonlinear model formulation as well as to keep the system in a valid operation region.

4. RESULTS

In this section, observers and feedback algorithms are applied to the nonlinear model (Neugebauer et al., 2018). Therefore, the partial differential equation characterizing the dynamics of the particle size density distribution (1) is transformed into a set of ordinary differential equations using a finite volume scheme. The resulting system comprising the latter as well as the ODEs describing the thermal conditions in the fluidization chamber have been solved numerically in MATLAB 2018a using the routine *ode15s* for numerical solution of the ordinary differential equation system. Furthermore, it is assumed that measurement noisy measurements are smoothed with a convenient technique before being processed further. For the design of the observer gains and integral state feedback the MATLAB function *lqr* was applied. In contrast, numerical studies using pole-placement in MATLAB via *place* have shown to to result in unstable estimation and control error dynamics.

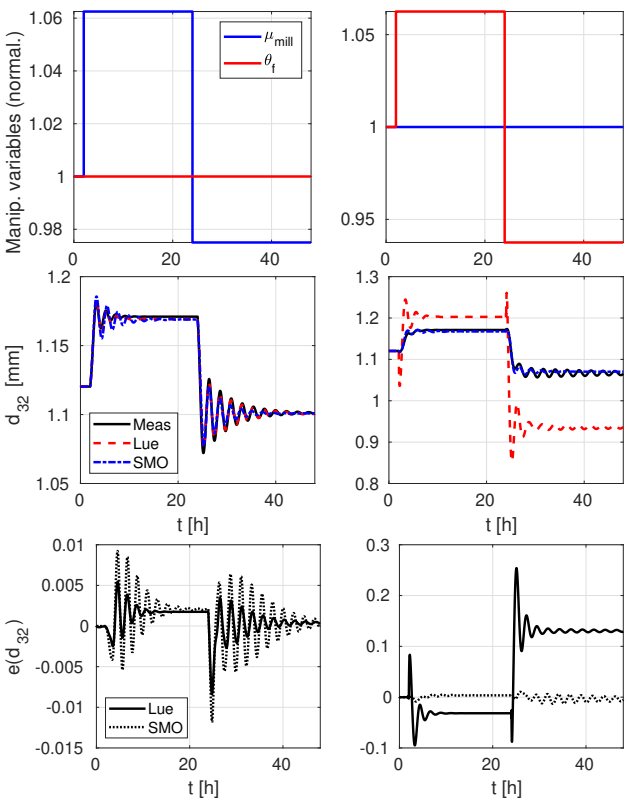

Fig. 3. *Performance of Luenberger and sliding mode observer for test scenarios: (left) change of milling diameter, (right) change of gas temperature*

4.1 Estimator performance

Performance of both observers is shown in Fig. 3 for two scenarios. In the first scenario on the left, the process is run in the nominal operation point of the manipulated variables (5). Afterwards, at $t = 2$ (24) h the milling diameter is varied to $\mu_{mill} = 0.85$ (0.78) mm while the drying gas temperature θ_f is kept constant. It is seen that the Luenberger observer is able to provide a good reconstruction of the unmeasured Sauter mean diameter. In comparison, the performance of the sliding mode observer is slightly worse, but the estimation error $e(d_{32}) = d_{32} - \hat{d}_{32}$ is still within a rather small range. On the right side of Fig. 3 the results for the second scenario are depicted. Here, the milling diameter μ_{mill} is kept constant while the temperature of the fluidization gas is changed at $t = 2$ (24) h to $\theta_f = 85$ (75) °C. In contrast to the first scenario, it is seen that the Luenberger observer performs worse compared to the sliding mode observer and is not able to deliver a reliable reconstruction of the unmeasured system output. One possible reason for this behavior could lie in the validity of the linearization within a close range around the operation point. For larger perturbations, the linear system is not able to account for the interaction between the outputs of both systems described in the full nonlinear model.

4.2 Inferential output feedback control

Performance of the PI-controller for both cases, based on direct measurement of d_{32} and based on its reconstruction

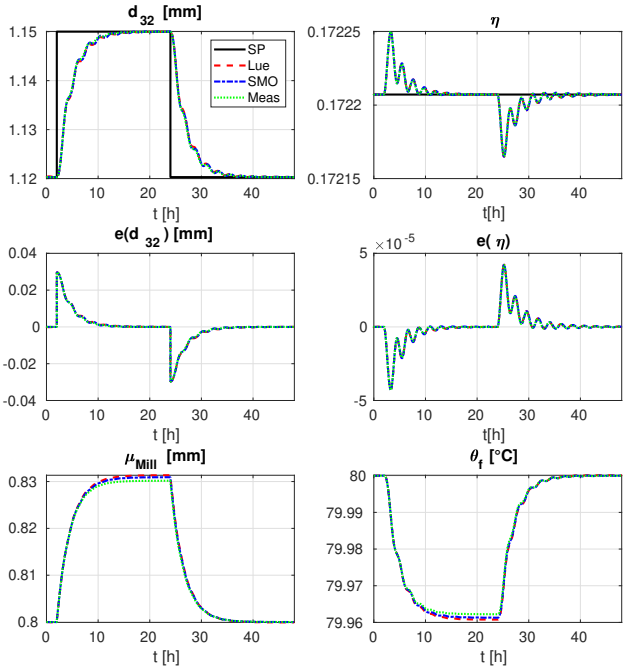

Fig. 4. *Output feedback based on measurement (Mea) or reconstruction of Sauter-mean-diameter d_{32} with sliding mode observer (SMO) / Luenberger observer (Lue)*

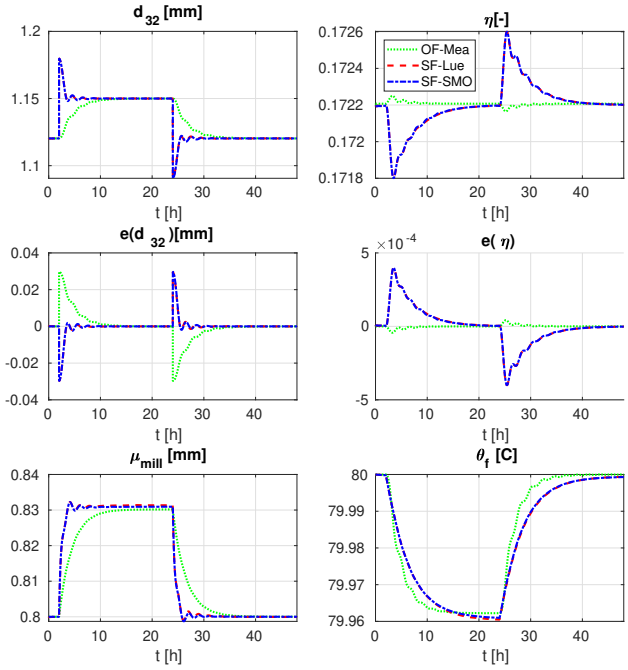

Fig. 5. *Output feedback using full measurement (OF-Mea) and integral state feedback control based on reconstruction of Sauter-mean-diameter d_{32} with sliding mode observer (SF-SMO) / Luenberger observer (SF-Lue)*

$\widehat{d}_{32}$ by Luenberger- and sliding mode observers is shown in Fig. 4. At $t = 2$ h the reference value of the Sauter mean diameter is increased while the drying potential reference is kept constant. It is seen that control using the observer estimate of the Sauter mean diameter allow nearly the same performance as using full measurement information. This comes rather unsurprisingly taking into account the estimation quality discussed in the previous section.

4.3 Inferential integral state feedback control

In Fig. 5 results are shown for integral state feedback control. Compared to output feedback based on measurements, the LQ-regulator drives the Sauter mean diameter faster to the desired reference value. Performance with respect to the drying potential is worse than under output feedback, yet the maximum errors are still relatively small.

5. SUMMARY

Close monitoring of specific particle properties is an important prerequisite for the production of high quality granules in particle formulation processes like fluidized bed layering granulation. It has to be emphasized that model-based concepts, in particular for FBLG processes, are far from being an everyday standard in industrial application: Here, heuristic control concepts based on years of trial-and-error experience which also require experienced technicians are still common practice. The aim of this study has been to show the general feasibility of model-based estimation and inferential control to such processes to (I) Obtain reliable information on non-measurable characteristics which are crucial for the process operation as well as product quality and (II) Actively use the gained model-based information online for efficient manipulation of the process.

In this manuscript, observers were formulated and evaluated for a nonlinear model of fluidized bed layering granulation presented by Neugebauer et al. (2018). The designed Luenberger and sliding mode observers were based on a numerical linearization of the complex nonlinear distributed plant dynamics. It was shown for two different scenarios that a sliding mode observer is able to accurately reconstruct the unmeasured particle property while the Luenberger observer fails in the second scenario. The simulation results thereby indicate that the linearized dynamics which were used for the observer/controller design, does only accurately represent the nonlinear process dynamics in a very narrow region around the nominal operation point. In the second scenario, the system seem not to be in this vicinity, explaining the worsened performance of Luenberger observer due to the resulting plant-model mismatch. The simulations on the other hand also suggest that the sliding mode observer is more robust with respect to such errors and thus represents the better option to cope with those. Though, the plant-model mismatch for the presented case results from linearization of the complex model, a comparable behavior of both observers is conjectured for general modeling errors. However, this rather general statement will have to be analyzed and specified in more detailed studies in future research for specific FBLG processes. Another important point for further analysis is concerned with the effects of measurement noise: So far, it was assumed that any noise in the measurements is smoothed out before further use for estimation/control. Obviously, in a more general approach convenient techniques, e.g. Extended or Unscented Kalman Filtering,

could be applied to directly process noisy measurements. However, the simulation results show that both observers are a sound base for the application of general output feedback controllers and (linear) integral state feedback controllers to obtain a desired product quality in terms of the product particles' Sauter mean diameter.

Future work will also focus on validation of the presented model-based observers for a pilot-scale-plant as described by Neugebauer et al. (2019) and application to related particle formation processes like spray fluidized bed spray agglomeration (Golovin et al., 2018). Of course, application of state observers facilitate implementation of advanced state-space control methods such as linear model predictive control (Bück et al., 2016), which may prove beneficial. Moreover, application of distributed parameter state estimation methods to the full nonlinear complex model will be researched (Dürr and Waldherr, 2018; Küper et al., 2019). Reconstruction of full number density distribution from available and reliable measurements enables application of advanced nonlinear distributed parameter control approaches (Palis and Kienle, 2014).

ACKNOWLEDGEMENTS

This project received funding by the *European Regional Development Fund* (ERDF) project *Center of Dynamic Systems* (CDS). The financial support is hereby gratefully acknowledged.

REFERENCES

Aström, K.J. and Murray, R.M. (2010). *Feedback systems: an introduction for scientists and engineers*. Princeton university press.

Bück, A., Dürr, R., Schmidt, M., and Tsotsas, E. (2016). Model predictive control of continuous layering granulation in fluidised beds with internal product classification. *Journal of Process Control*, 45, 65–75.

Cotabarren, I.M., Bertn, D.E., Bucal, V., and Pia, J. (2015). Feedback control strategies for a continuous industrial fluidized-bed granulation process. *Powder Technology*, 283, 415 – 432.

Dürr, R. and Waldherr, S. (2018). A novel framework for parameter and state estimation of multicellular systems using gaussian mixture approximations. *Processes*, 6(10).

Golovin, I., Strenzke, G., Dürr, R., Palis, S., Bück, A., Tsotsas, E., and Kienle, A. (2018). Parameter identification for continuous fluidized bed spray agglomeration. *Processes*, 6(12).

Küper, A., Dürr, R., and Waldherr, S. (2019). Dynamic density estimation in heterogeneous cell populations. *IEEE Control Systems Letters*, 3(2), 242–247.

Litster, J. and Ennis, B. (2004). *The Science and Engineering of Granulation Processes*. Springer Netherlands.

Mohd Ali, J., Ha Hoang, N., Hussain, M., and Dochain, D. (2015). Review and classification of recent observers applied in chemical process systems. *Computers and Chemical Engineering*, 76, 27–41.

Mörl, L., Heinrich, S., and Peglow, M. (2007). Chapter 2 fluidized bed spray granulation. In A. Salman, M. Hounslow, and J. Seville (eds.), *Granulation*, volume 11 of *Handbook of Powder Technology*, 21–188. Elsevier Science B.V.

Neugebauer, C., Diez, E., Bück, A., Palis, S., Heinrich, S., and Kienle, A. (2019). On the dynamics and control of continuous fluidized bed layering granulation with screen-mill-cycle. *Powder Technology*, 354, 765–778.

Neugebauer, C., Bück, A., Palis, S., Mielke, L., Tsotsas, E., and Kienle, A. (2018). Influence of thermal conditions on particle properties in fluidized bed layering granulation. *Processes*, 6(12).

Neugebauer, C., Bck, A., and Kienle, A. (2020). Control of particle size and porosity incontinuous fluidized-bed layering granulation processes. *Chemical Engineering & Technology*, 43(5), 813–818.

Palis, S. and Kienle, A. (2014). Discrepancy based control of particulate processes. *Journal of Process Control*, 24(3), 33 – 46.

Ramkrishna, D. (2000). *Population Balances: Theory and Applications to Particulate Systems in Engineering*. Academic Press, San Diego.

Rieck, C., Hoffmann, T., Bück, A., Peglow, M., and Tsotsas, E. (2015). Influence of drying conditions on layer porosity in fluidized bed spray granulation. *Powder Technology*, 272, 120–131.

Shtessel, Y., Edwards, C., Fridman, L., and Levant, A. (2014). *Sliding mode control and observation*, volume 10. Springer.

Simon, D. (2006). *Optimal state estimation: Kalman, H infinity, and nonlinear approaches*. John Wiley & Sons.

Skogestad, S. and Postlethwaite, I. (2007). *Multivariable feedback control: analysis and design*, volume 2. Wiley New York.

van Meel, D. (1958). Adiabatic convection batch drying with recirculation of air. *Chemical Engineering Science*, 9(1), 36–44.